

A PPO-Based Bitrate Allocation Conditional Diffusion Model for Remote Sensing Image Compression

Yuming Han, *Graduate Student Member, IEEE*, Jooho Kim, Anish Shakya, *Graduate Student Member, IEEE*

Abstract—Existing remote sensing image compression methods still explore to balance high compression efficiency with the preservation of fine details and task-relevant information. Meanwhile, high-resolution drone imagery offers valuable structural details for urban monitoring and disaster assessment, but large-area datasets can easily reach hundreds of gigabytes, creating significant challenges for storage and long-term management. In this paper, we propose a PPO-based bitrate allocation Conditional Diffusion Compression (PCDC) framework. PCDC integrates a conditional diffusion decoder with a PPO-based block-wise bitrate allocation strategy to achieve high compression ratios while maintaining strong perceptual performance. We also release a high-resolution drone image dataset with richer structural details at a consistent low altitude over residential neighborhoods in coastal urban areas. Experimental results show compression ratios of $19.3\times$ on DIV2K and $21.2\times$ on the drone image dataset. Moreover, downstream object detection experiments demonstrate that the reconstructed images preserve task-relevant information with negligible performance loss.

Index Terms—Remote sensing, image compression, diffusion model, reinforcement learning, object detection.

I. INTRODUCTION

With the ongoing advances in remote sensing (RS) technology, the volume of imagery collected by modern aerial platforms, especially unmanned aerial vehicles (UAVs), is increasing dramatically [1]. This growth is fueled by the rapid adoption of high resolution sensors and more frequent data acquisition, which together produce massive datasets with rich spatial details [2]. Efficient compression is therefore essential for reducing storage overhead and easing the burden of data management, while also enabling more scalable post collection processing [3]. Traditional image compression methods, such as JPEG2000 [4] and BPG [5], have been widely adopted in remote sensing workflows. However, applying traditional codecs to drone based remote sensing imagery has three key limitations. First, remote sensing images contain dense textures, sharp edges, and strong scale variation, making them difficult to compress effectively with fixed transforms and uniform quantization [6]. Second, traditional compression is mainly optimized for pixel level reconstruction quality [5], which does not preserve the most task relevant information. Third, at low bitrates, traditional codecs introduce visible distortions and lose fine structures that are critical for remote sensing analysis [7].

Yuming Han is with the Department of Electrical and Computer Engineering, Texas A&M University, College Station, TX 77843 USA (e-mail: yuminghan@tamu.edu).

Jooho Kim is with the Institute for a Disaster Resilient Texas, Texas A&M University, College Station, TX 77843 USA (e-mail: Jooho.kim@tamu.edu).

Anish Shakya is with Department of Marine & Coastal Environmental Science, Texas A&M University, Galveston, TX 77554 USA (anish_shakya@tamu.edu).

To overcome the limitations of traditional methods, recent studies have explored neural network based compression, such as convolutional neural network (CNN) [8], Transformer [9], and generative adversarial network (GAN) [10] architectures. However, these approaches still suffer from three limitations in remote sensing image compression: (i) deterministic single pass decoding limits error correction and causes over smoothing [8]; (ii) fixed rate distortion objectives impose a rigid tradeoff between fidelity and perceptual quality [8], [9]; and (iii) reconstruction quality degrades rapidly at very low bitrates, leading to detail loss or unstable textures [10]. To address these limitations, diffusion models (DMs) [11] have been introduced into learned image compression as a new class of generative decoders. Diffusion based reconstruction proceeds via iterative denoising, which provides a natural mechanism to correct quantization induced errors and recover missing structures [12]. Moreover, the sampling process enables more flexible control of the fidelity realism tradeoff, helping reduce over smoothing and suppress unnatural artifacts [13]. Since these models operate in pixel space, the cost of inference is high due to sequential evaluation. The latent diffusion model (LDM) [14] was introduced to reduce computational costs by performing diffusion and reverse steps in the latent space. However, the decoding complexity and computational cost remain high for large scale RS datasets.

Beyond technical performance, the effect of compression on downstream tasks is also critical in remote sensing, since decompressed images are used for applications such as object detection and scene understanding [15]. However, most existing studies focus mainly on rate distortion or perceptual quality, while downstream task performance remains underexplored. Therefore, to address the problems above, we present a diffusion model based and downstream task friendly drone image compression model. The primary contributions of this article can be summarized as follows.

- **Conditional Diffusion Compression Framework:** We propose a PPO-based bitrate allocation Conditional Diffusion Compression (PCDC) framework that considers both reconstruction fidelity and downstream task utility. Numerical results show that we achieve $19.3\times$ compression on DIV2K and $21.2\times$ on the drone image dataset.
- **PPO-based Bitrate Allocation:** We design a novel PPO-Lagrangian controller performs block-wise bitrate allocation using high-frequency residual and CNN encoder features as state inputs. The policy selects allocation levels for each block under a global bitrate constraint, achieving superior perceptual performance while maintaining the target compression ratio.

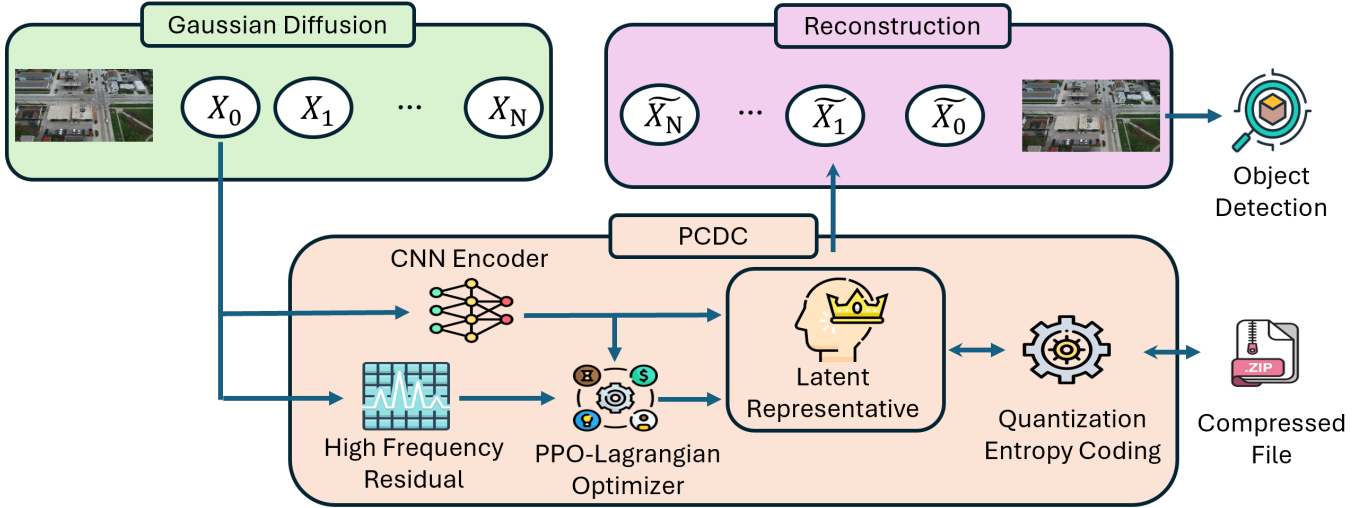


Fig. 1. System model of the proposed diffusion-based image compression framework with PPO-based bitrate allocation.

- **Object Detection on Self-collected Dataset:** We release a drone image dataset consisting of high-resolution nadir images captured at a low altitude with richer structural details in coastal urban areas. Furthermore, downstream object detection results show negligible differences between the original and reconstructed images, demonstrating that the PCDC effectively preserves task-relevant information.

The rest of this article is organized as follows. Section II presents the system model, Section III reports the experimental results, and Section IV concludes the article.

II. SYSTEM MODEL

A. Conditional Diffusion Based Compression Framework

The proposed framework follows the context-dependent compression paradigm [12], where the image is first encoded into a latent representation and subsequently reconstructed using a conditional diffusion model. The latent representation captures the global structural and semantic information of the image, while the diffusion model reconstructs the image through iterative denoising conditioned on this latent description. Given the input image $x_0 \in \mathbb{R}^{H \times W \times 3}$, a CNN encoder extracts a latent representation that summarizes the image content as $\mathbf{z} = \text{Enc}(x_0)$, where $\text{Enc}(\cdot)$ denotes the encoder network. The latent variable \mathbf{z} captures the essential spatial structures and contextual information required for image reconstruction while reducing redundancy in the input image.

To enable efficient transmission, the latent representation is quantized using element-wise rounding $\hat{\mathbf{z}} = \text{round}(\mathbf{z})$. The quantized latent $\hat{\mathbf{z}}$ is then entropy-coded under a learned probability model $p(\hat{\mathbf{z}})$. The expected bitrate required to encode the latent representation is therefore given by

$$R_{\text{base}} = \mathbb{E}[-\log_2 p(\hat{\mathbf{z}})]. \quad (1)$$

The compressed bitstream corresponding to $\hat{\mathbf{z}}$ forms the compact representation of the input image and serves as the conditioning signal for the subsequent reconstruction process.

Unlike traditional neural compression systems that employ deterministic decoders, the proposed framework reconstructs

the image using a conditional diffusion model. Diffusion models generate samples by reversing a gradual noising process through a sequence of denoising steps. The forward diffusion process progressively perturbs the clean image by adding Gaussian noise as $x_n = \sqrt{\alpha_n} x_0 + \sqrt{1 - \alpha_n} \epsilon$, where $\epsilon \sim \mathcal{N}(0, I)$ and $\{\alpha_n\}_{n=1}^N$ defines a predefined variance schedule. During reconstruction, the reverse diffusion process iteratively removes noise to recover the image. The reverse transition is conditioned on the transmitted latent representation $\hat{\mathbf{z}}$. In practice, the diffusion model is implemented using a U-Net architecture where the latent representation is injected as a conditioning signal to guide the reconstruction process.

B. PPO-based Bitrate Allocation

We further propose a constrained deep reinforcement learning strategy to adapt block-wise bit allocation, while satisfying a target compression-ratio constraint. Unlike [13], our encoder does *not* run the diffusion decoder and thus cannot access reconstruction errors. Instead, the policy relies only on available signals: (i) a high-frequency residual map extracted from the input image, and (ii) block-level CNN encoder features. The learned policy outputs block-wise allocation decisions that control local detail preservation during quantization and entropy coding under a global bitrate budget.

First, the encoder computes a high-frequency residual map as $h = \mathcal{H}(x_0)$, where $\mathcal{H}(\cdot)$ is a fixed high-pass filter. We partition the image into B non-overlapping blocks $\{\mathcal{B}_b\}_{b=1}^B$. For each block b , the policy selects an allocation action α_b controlling local detail preservation. For stability and codec compatibility, we adopt a discrete action space

$$\beta_b \in \mathcal{A} = \{a_1, \dots, a_K\}, \quad \beta = \{\beta_b\}_{b=1}^B. \quad (2)$$

Since the state is constructed from encoder-side observables. At step b , we define

$$s_b = \left[\Phi_h(h|_{\mathcal{B}_b}); \Phi_{\mathbf{z}}(\mathbf{z}|_{\mathcal{B}_b}); \rho_b; p_b \right], \quad (3)$$

where $\Phi_h(\cdot)$ denotes block statistics of the high-frequency residual, $\Phi_{\mathbf{z}}(\cdot)$ is a pooled CNN embedding for the block,

ρ_b is the normalized remaining bitrate budget, and p_b includes block coordinates. We further apply action masking based on the remaining budget to prevent infeasible allocations.

Next, let $R_b(\alpha_b)$ denote the incremental bit cost induced by selecting action α_b for block b . The total bitrate is

$$R_{\text{tot}}(\boldsymbol{\alpha}) = R_{\text{base}} + \sum_{b=1}^B R_b(\beta_b). \quad (4)$$

The target compression-ratio requirement is enforced by a hard bitrate constraint $R_{\text{tot}}(\boldsymbol{\alpha}) \leq R_{\text{max}}$. The diffusion decoder produces a reconstruction \tilde{x} . Although the decoder is not invoked in the forward encoder pipeline, it is used to compute learning feedback. We define a utility combining fidelity and perceptual metrics:

$$U(x_0, \tilde{x}_0) = -\lambda_p D(x_0, \tilde{x}_0) - \lambda_s (1 - \text{SSIM}(x_0, \tilde{x}_0)) - \lambda_l \text{LPIPS}(x_0, \tilde{x}_0) - \lambda_d \text{DISTS}(x_0, \tilde{x}_0), \quad (5)$$

where $D(\cdot, \cdot)$ is the mean squared error, $\text{SSIM}(\cdot, \cdot)$ denotes the structural similarity index measure, $\text{LPIPS}(\cdot, \cdot)$ is the learned perceptual image patch similarity, and $\text{DISTS}(\cdot, \cdot)$ denotes the deep image structure and texture similarity. To satisfy the bitrate constraint, we optimize a Lagrangian reward:

$$r = U(x_0, \tilde{x}_0) - \eta (R_{\text{tot}}(\boldsymbol{\beta}) - R_{\text{max}}), \quad (6)$$

with dual variable $\eta \geq 0$. The constrained objective is

$$\max_{\pi_\theta} \mathbb{E}_{\pi_\theta} [U(x_0, \tilde{x}_0)] \quad \text{s.t.} \quad \mathbb{E}_{\pi_\theta} [R_{\text{tot}}(\boldsymbol{\beta})] \leq R_{\text{max}}. \quad (7)$$

We solve it by alternating policy optimization and dual ascent:

$$\eta \leftarrow \left[\eta + \rho (R_{\text{tot}}(\boldsymbol{\beta}) - R_{\text{max}}) \right]_+, \quad (8)$$

where ρ is a stepsize and $[\cdot]_+ = \max(\cdot, 0)$. This is well suited to the non-monotonic behavior observed in practice, where increasing allocation does not improve perceptual quality.

Last, we parameterize the policy by $\pi_\theta(a_b|s_b)$ and learn a value function $V_\psi(s_b)$. Each episode corresponds to B sequential block decisions. After sampling actions $\{\beta_b\}$ and producing the bitstream, we decode and reconstruct \tilde{x} to compute the terminal reward r . Let $G_b = r$ denote the return from step b . The advantage estimate is

$$A_b = G_b - V_\psi(s_b). \quad (9)$$

We define the likelihood ratio $\varrho_b(\theta) = \frac{\pi_\theta(a_b|s_b)}{\pi_{\theta_{\text{old}}}(a_b|s_b)}$. The PPO clipped surrogate objective is

$$\begin{aligned} \mathcal{L}_{\text{PPO}}(\theta) = \mathbb{E} \left[\min \left(\varrho_b(\theta) A_b, \text{clip}(\varrho_b(\theta), 1 - \gamma, 1 + \gamma) A_b \right) \right] \\ + \kappa \mathbb{E} [H(\pi_\theta(\cdot|s_b))], \end{aligned} \quad (10)$$

where γ is the clipping parameter, $H(\cdot)$ denotes entropy, and κ controls exploration. At test time, we perform a small number of PPO updates per image, followed by the dual update in (8). This online adaptation allows the policy to adjust its allocation strategy to the drone images while maintaining the compression constraint through the Lagrangian mechanism. Overall, we outline PPO-Based bitrate allocation in Algorithm 1.

Algorithm 1 PPO-Based Bitrate Allocation

Require: Image x_0 ; HF extractor \mathcal{H} ; blocks $\{\mathcal{B}_b\}_{b=1}^B$; actions \mathcal{A} ; bitrate constraint R_{max} ; policy π_θ ; value V_ψ ; dual η .

- 1: **for** each test image x_0 **do**:
- 2: Compute $h \leftarrow \mathcal{H}(x)$; initialize ρ_b .
- 3: **for** $b = 1$ to B **do**:
- 4: Form $s_b = [\Phi_h(h|_{\mathcal{B}_b}); \Phi_z(\mathbf{z}|_{\mathcal{B}_b}); \rho_b; p_b]$.
- 5: Sample $\beta_b \sim \pi_\theta(\cdot|s_b)$; update ρ_b .
- 6: **end for**
- 7: Encode to obtain R_{tot} ; decode to obtain \tilde{x}_0 .
- 8: Compute utility U via (5).
- 9: Compute reward r by (6) and advantages A_b by (9).
- 10: Update π_θ with (s_b, β_b, A_b) ; update η via (8).
- 11: **end for**

III. NUMERICAL RESULTS

A. Experiments Setup

We evaluate the proposed method on both public DIV2K dataset and our self-collected drone image dataset. We make this dataset publicly available at [16]. The drone image dataset contains 100 RGB images captured at an altitude of around 47.01 m over urban areas in Galveston, Texas, with a high-resolution of 5472×3648 . As shown in Fig. 2, it includes nadir views of buildings, roads, parking areas, and vehicles, covering scene characteristics that are not well represented in existing open-source datasets [17], [18]. Each image is



Fig. 2. Data collection points and sample images in Galveston, Texas.

partitioned into 16×16 blocks. The PPO controller uses a discrete action space with $K = 5$ allocation levels to control the preservation strength of each block under bitrate constraint R_{max} , corresponding to a compression ratio of 0.2. The policy is trained with clipping parameter $\gamma = 0.2$, entropy weight $\kappa = 0.01$, actor learning rate 3×10^{-4} , and critic learning rate 10^{-3} . The Lagrange multiplier is updated with step size $\rho = 10^{-3}$. The reward is weighted by $\lambda_p = 1.0$, $\lambda_s = 0.5$, $\lambda_l = 0.2$, and $\lambda_d = 0.2$, respectively.

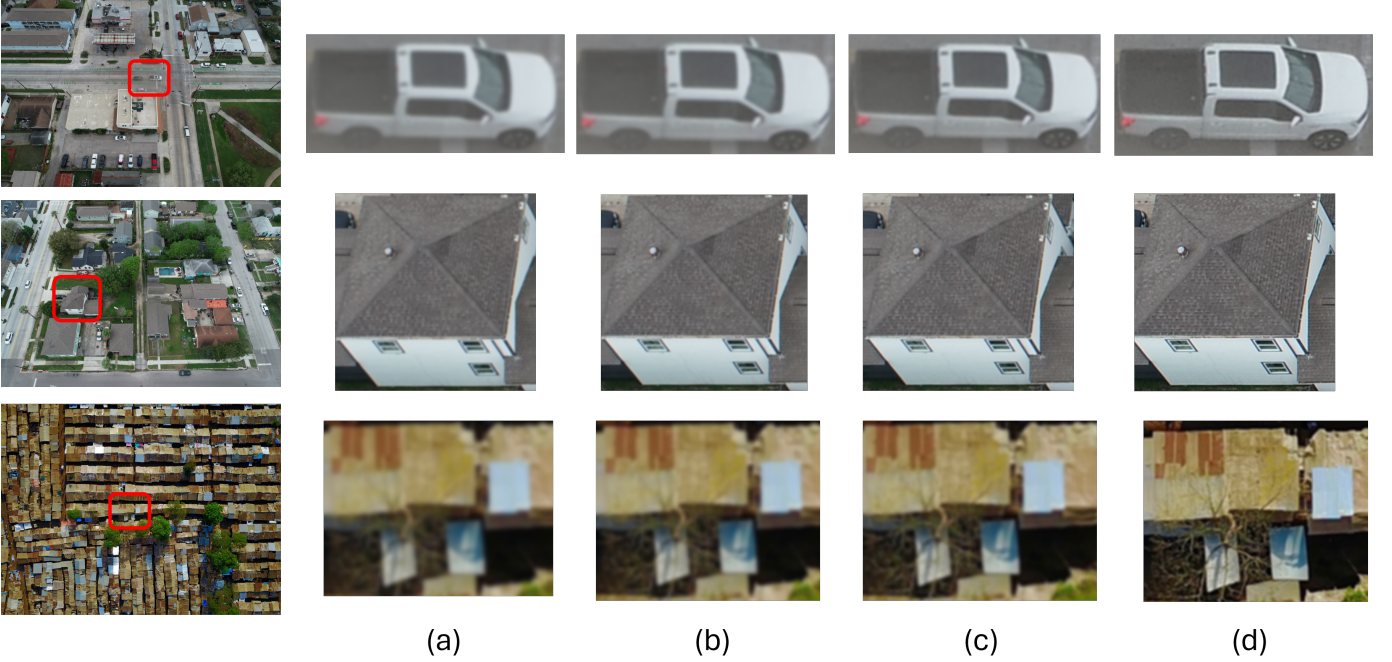


Fig. 3. Visual comparison of reconstruction images by different methods. The first two rows are from the proposed drone image dataset and the last row is from DIV2K. (a) BPG, (b) HiFiC, (c) CDC, and (d) the proposed PCDC. The proposed method reconstructs sharper edges and clearer structural details.

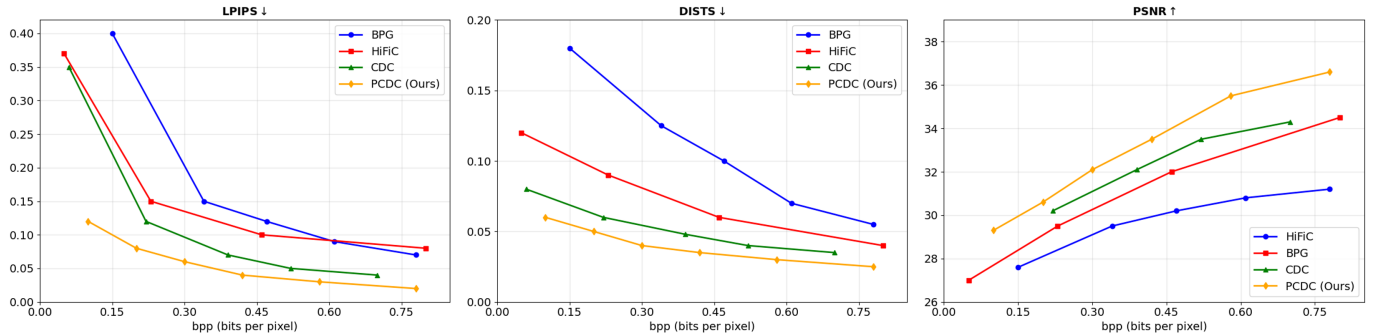


Fig. 4. Rate–distortion comparison of BPG, HiFiC, CDC, and the proposed PCDC in terms of LPIPS, DISTs, and PSNR across different bitrates (bpp).

TABLE I
COMPRESSION RATIO COMPARISON ON DIV2K AND DRONE IMAGE DATASETS.

Model	DIV2K	Drone Image Dataset
BPG	10.8	11.6
HiFiC	15.9	16.8
CDC	16.4	17.2
PCDC (Ours)	19.3	21.2

B. Comparison Results

We compare our method to BPG [5], HiFiC [10] and CDC [12]. First, Table I shows that the PCDC achieves the highest compression ratio on both datasets. In comparison, BPG yields the lowest compression efficiency, while the learned compression methods HiFiC and CDC provide moderate improvements but remain close to each other. This trend indicates that diffusion-based compression frameworks already offer advantages over traditional codecs, and the proposed

enhancements in PCDC further improve coding efficiency. Moreover, all methods achieve higher compression ratios on the drone image dataset, suggesting that aerial imagery with larger homogeneous regions and repetitive structures is more compressible than the diverse natural scenes. Fig. 3 further provides a visual comparison on reconstruction images.

Next, Fig 4 compares the rate–distortion performance of different methods in terms of LPIPS, DISTs, and PSNR across varying bitrates. The proposed PCDC consistently achieves the best performance among all methods. These results demonstrate that the proposed framework effectively improves both perceptual fidelity and reconstruction accuracy. Moreover, since the PPO-based bitrate allocation is introduced as an add-on to the conditional diffusion compression model, the performance gap between CDC and PCDC can be interpreted as an ablation result. The consistent improvement of PCDC over CDC demonstrates that the proposed bitrate allocation strategy enhances coding efficiency and reconstruction quality beyond the conditional diffusion framework alone.

C. Downstream Object Detection Performances

For further demonstrating the effectiveness of the proposed model, we perform an object detection downstream task using both pretrained YOLO models (YOLO-pre) and fine-tuned YOLO models (YOLO-ft). We fine-tune the model using an independent drone image dataset separate from the testing set, which includes building labels. Table II reports the detection performance on the original and reconstructed images in terms of the building ratio (B-R), vehicle ratio (V-R), confidence score (Conf.), and intersection over union (IoU), where B and V denote building and vehicle, respectively. Fig. 5

TABLE II
DETECTION RESULTS ON ORIGINAL AND RECONSTRUCTED IMAGES.

Model	Data	B-R	V-R	Conf.	IoU
YOLO11s-pre	Ori.	–	0.99	V: 0.825	V: 0.97
	Rec.	–	0.98	V: 0.828	V: 0.97
YOLO11s-ft	Ori.	1.02	0.96	B: 0.789, V: 0.743	B: 0.95, V: 0.96
	Rec.	1.00	0.95	B: 0.789, V: 0.740	B: 0.95, V: 0.96
YOLO12s-pre	Ori.	–	0.96	V: 0.840	V: 0.97
	Rec.	–	0.95	V: 0.840	V: 0.97
YOLO12s-ft	Ori.	0.98	0.89	B: 0.753, V: 0.719	B: 0.96, V: 0.96
	Rec.	0.96	0.88	B: 0.751, V: 0.718	B: 0.96, V: 0.96

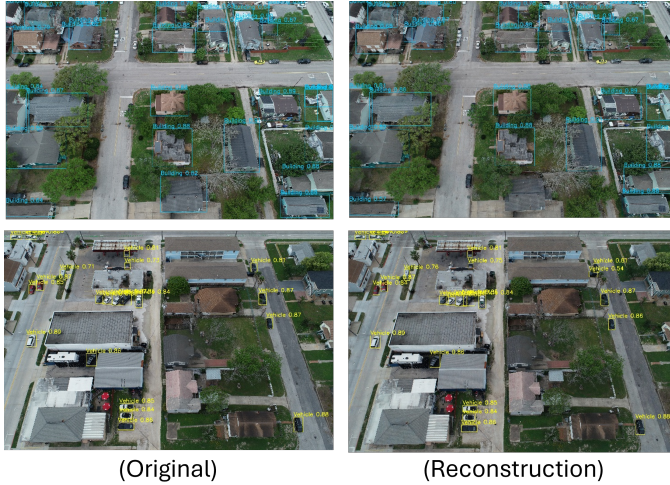


Fig. 5. Visual comparisons with corresponding confidence scores for building (first row) and vehicle (second row) detections.

further provides a visual comparison with confidence score on vehicles and buildings. These negligible average differences of around 0.02 in Table II indicate that the proposed compression framework preserves important semantic structures and object-level features, allowing downstream detection tasks to maintain comparable performance after reconstruction.

IV. CONCLUSION

In this paper, we proposed PCDC, a conditional diffusion-based framework for RS image compression that preserves reconstruction quality and downstream task utility. With a novel PPO-based bitrate allocation strategy, PCDC achieves high compression ratios while maintaining strong perceptual

performance. In addition, we release a high-resolution drone image dataset and demonstrate through downstream object detection experiments that the reconstructed images preserve task-relevant information with negligible performance loss. These results suggest that PCDC can support efficient storage planning and long-term data management by reducing the storage costs associated with large-scale drone imagery archives. Future work will extend the framework to more remote sensing tasks and investigate more efficient diffusion sampling for practical deployment.

REFERENCES

- [1] Q. Hu, C. Wu, Y. Wu, and N. Xiong, "Uav image high fidelity compression algorithm based on generative adversarial networks under complex disaster conditions," *IEEE Access*, vol. 7, pp. 91 980–91 991, 2019.
- [2] H. Fang, S. Guo, X. Wang, S. Liu, C. Lin, and P. Du, "Automatic urban scene-level binary change detection based on a novel sample selection approach and advanced triplet neural network," *IEEE Transactions on Geoscience and Remote Sensing*, vol. 61, pp. 1–18, 2023.
- [3] T. Pan, L. Zhang, L. Qu, and Y. Liu, "A coupled compression generation network for remote-sensing images at extremely low bitrates," *IEEE Transactions on Geoscience and Remote Sensing*, vol. 61, pp. 1–14, 2023.
- [4] D. S. Taubman, M. W. Marcellin, and M. Rabbani, "Jpeg2000: Image compression fundamentals, standards and practice," *Journal of Electronic Imaging*, vol. 11, no. 2, pp. 286–287, 2002.
- [5] F. Bellard, "Bpg image format," <http://bellard.org/bpg/>, 2018, accessed: 2018.
- [6] Z. Xing, S. Yang, X. Zan, X. Dong, Y. Yao, Z. Liu, and X. Zhang, "Flood vulnerability assessment of urban buildings based on integrating high-resolution remote sensing and street view images," *Sustainable Cities and Society*, vol. 92, p. 104467, 2023.
- [7] T. Pan, L. Zhang, Y. Song, and Y. Liu, "Hybrid attention compression network with light graph attention module for remote sensing images," *IEEE Geoscience and Remote Sensing Letters*, vol. 20, pp. 1–5, 2023.
- [8] Z. Tang, H. Wang, X. Yi, Y. Zhang, S. Kwong, and C.-C. J. Kuo, "Joint graph attention and asymmetric convolutional neural network for deep image compression," *IEEE Transactions on Circuits and Systems for Video Technology*, vol. 33, no. 1, pp. 421–433, 2022.
- [9] B. Li, J. Liang, and J. Han, "Variable-rate deep image compression with vision transformers," *IEEE Access*, vol. 10, pp. 50 323–50 334, 2022.
- [10] F. Mentzer, G. D. Toderici, M. Tschannen, and E. Agustsson, "High-fidelity generative image compression," *Advances in Neural Information Processing Systems*, vol. 33, 2020.
- [11] J. Ho, A. Jain, and P. Abbeel, "Denoising diffusion probabilistic models," *arXiv preprint arxiv:2006.11239*, 2020.
- [12] R. Yang and S. Mandt, "Lossy image compression with conditional diffusion models," *Advances in Neural Information Processing Systems*, vol. 36, pp. 64 971–64 995, 2023.
- [13] N. F. Ghose, J. Petersen, A. Wiggers, T. Xu, and G. Sautiere, "A residual diffusion model for high perceptual quality codec augmentation," *arXiv preprint arXiv:2301.05489*, 2023.
- [14] R. Rombach, A. Blattmann, D. Lorenz, P. Esser, and B. Ommer, "High-resolution image synthesis with latent diffusion models," in *Proceedings of the IEEE/CVF conference on computer vision and pattern recognition*, 2022, pp. 10 684–10 695.
- [15] S. Li, Z. Zhou, M. Zhao, J. Yang, W. Guo, Y. Lv, L. Kou, H. Wang, and Y. Gu, "A multitask benchmark dataset for satellite video: Object detection, tracking, and segmentation," *IEEE Transactions on Geoscience and Remote Sensing*, vol. 61, pp. 1–21, 2023.
- [16] Disaster Data Reconnaissance Center at the Institute for a Disaster Resilient Texas, "High resolution low altitude drone remote sensing dataset," 2026. [Online]. Available: <https://huggingface.co/datasets/yuminghan12123/Low-Altitude-Drone-Remote-Sensing-Dataset>
- [17] P. Zhu, L. Wen, D. Du, X. Bian, H. Fan, Q. Hu, and H. Ling, "Detection and tracking meet drones challenge," *IEEE transactions on pattern analysis and machine intelligence*, vol. 44, no. 11, pp. 7380–7399, 2021.
- [18] Esri, "Drone data: Download sample drone datasets," n.d. [Online]. Available: <https://www.esri.com/en-us/arcgis/products/arcgis-reality/resources/sample-drone-datasets>